Journal of Power Sources 225 (2013) 113–118

Contents lists available at SciVerse ScienceDirect

Journal of Power Sources

journal homepage: www.elsevier.com/locate/jpowsour

1-Ethyl-1-methyl piperidinium bis(trifluoromethanesulfonyl)imide as a co-solvent in Li-ion batteries

Ketack Kim [a,*], Young-Hyun Cho [b], Heon-Cheol Shin [c]

[a] Department of Chemistry, Sangmyung University, Seoul 110-743, Republic of Korea
[b] R&D team, SB Limotive, Ulsan 689-811, Republic of Korea
[c] School of Materials Science and Engineering, Pusan National University, Busan 609-735, Republic of Korea

HIGHLIGHTS

- A solid ionic liquid (EMP-TFSI) was used as a new co-solvent for Li batteries.
- EMP-TFSI performed better as a co-solvent than MPP-TFSI.
- The 50 wt% EMP-TFSI electrolyte performed as well as a carbonate electrolyte.

ARTICLE INFO

Article history:
Received 9 August 2012
Received in revised form
27 September 2012
Accepted 12 October 2012
Available online 23 October 2012

Keywords:
Lithium-ion battery
Solid ionic liquid
Flame retardancy
Conductivity

ABSTRACT

1-Ethyl-1-methyl piperidinium bis(trifluoromethanesulfonyl)imide (EMP-TFSI) is an ionic liquid with a melting temperature of 85 °C. Although it is a solid salt, it shows good miscibility with carbonate solvents, which allows EMP-TFSI to be used as a co-solvent in these systems. Ethylene carbonate is another solid co-solvent used in Li-ion batteries. Due to its smaller cationic size, EMP-TFSI provides better conductivity as a co-solvent than 1-methyl-1-propyl piperidinium bis(trifluoromethanesulfonyl)imide (MPP-TFSI), which is the smallest room-temperature piperidinium liquid salt known. In cells with 50 wt% IL and 50 wt% carbonate electrolyte, an EMP-TFSI mixed electrolyte performs better than an MPP-TFSI mixed electrolyte. Additionally, the discharge capacity values obtained from rate capability tests carried out with mixed EMP-TFSI are as good as those conducted with a pure carbonate electrolyte.

1. Introduction

Flame retardancy is one of the most attractive properties of ionic liquids (ILs) for use in battery applications. When the flammable components of Li-ion batteries are replaced with ILs or less flammable materials, Li-ion batteries become significantly safer for use as large energy-storage devices in applications ranging from household use to area energy control. ILs have shown considerable potential not only as electrolytes [1–7] in Li-ion batteries but also as solvents for new binders [8] and as ionic conductors in solid electrolytes [9,10].

Room temperature ionic liquids (RTILs) are salts with melting temperatures below 100 °C [11,12]. Among RTILs, salts that are liquid at room temperature are more convenient to use than salts that are solid. The conductivities of imidazolium-based ILs are superior to those of other RTILs [13,14]. Their conductivities are as good as carbonate-based electrolytes in Li-ion batteries. However, their potential windows are not sufficiently wide for use in many Li-ion battery applications [6]. The structural modification of cations can result in new ILs with the ability to provide wider potential windows. However, modifications to alkyl branches in ILs can readily increase the cation sizes, which leads to low ion mobility, i.e., low conductivity. Among the modification attempts that have been made, modifications to ether groups on the alkyl branches have improved the conductivity to a measurable extent [6,15]. Most ILs perform poorly with graphite anodes, resulting in the electrolysis of the ILs [16,17] at the anode and/or the intercalation of the cations in the ILs [18,19]. To solve these problems, passivation layer-forming agents, such as vinylene carbonate (VC), carbonate solvents including ethylene carbonate (EC), or allyl-substituted ILs [20,21], have been added to increase the cycle life of the battery [13,16,22]. Additionally, ILs can face wettability problems associated with the separator in Li-ion batteries, not only because ILs are viscous but also because the ILs and the separators frequently possess different polarities [23]. Due to the many

* Corresponding author. Tel.: +82 2 781 7508; fax: +82 2 2287 0070.
E-mail address: ketack.kim@smu.ac.kr (K. Kim).

0378-7753/$ – see front matter © 2012 Elsevier B.V. All rights reserved.
http://dx.doi.org/10.1016/j.jpowsour.2012.10.038

obstacles presented by ILs, it is certain that the use of a pure IL alone as an electrolyte in Li-ion cells will cause several combined problems. Because the conventional carbonate electrolytes include multiple additives, a pure IL alone is not able to support the satisfactory operation of Li-ion batteries.

However, the wide potential window is another advantage of ILs over conventional electrolytes. ILs with pyrrolidinium and piperidinium have wide potential windows, which makes them promising candidates for applications in high-voltage Li batteries [24]. These ILs can expand their oxidation limit to 5 V versus Li^+/Li. Due to their wide potential limits, piperidinium and pyrrolidinium-TFSI have received considerable attention. Among those ILs, the cations that possess between 9 and 11 atoms have been the focus of extensive research efforts [22,24–29] because they demonstrate the best conductivity in this category of IL species due to their small cationic sizes.

In this study, we demonstrate that it is not necessary for the ILs used in Li-ion batteries to be liquids at room temperature. When an IL can be used as a binary solvent with a carbonate counterpart, ILs that melt above room temperature (RT) can be used as a co-solvent mixture to create a solution. Some ILs with melting temperatures above RT possess smaller cations than those of room-temperature liquid salts. Once the solid has been mixed with a carbonate solvent, the ILs with smaller ions dissolve. The smaller ions move more freely in the liquid than the larger ions, providing enhanced conductivity. An IL content greater than 30% in the electrolyte can lead to good flame retardancy or nonflammable properties [13]. Mixing the proper amount of IL with a carbonate electrolyte can provide improved safety while maintaining moderate Li-ion battery conductivity. Ethylene carbonate (EC), which is a common solvent for carbonate solvents in Li-ion batteries, is an example of a solid solvent component with the ability to form an electrolyte solution. Solid ILs can act as a co-solvent in liquid electrolytes. Binary solvents made with solid ILs represent another opportunity to blend ILs and carbonates to improve the conductivity of mixed ILs. Piperidinium cations were selected for our study due to their wide potential window, which is an inevitable requirement for high-voltage cathode materials, such as $LiNi_{0.5}Mn_{1.5}O_4$. The solid IL used in this study is 1-ethyl-1-methyl-piperidinium bis(trifluoromethanesulfonyl)imide (EMP-TFSI), which has not been reported previously in Li battery applications. 1-Methyl-1-propyl-piperidinium bis(trifluoromethanesulfonyl)imide (MPP-TFSI), the smallest RTIL in piperidinium-TFSI, is used for comparison purposes.

2. Experimental

2.1. Chemical and cell preparations

N-methylpiperidine (Aldrich, 99%), 1-bromopropane (Acros, 99%) and bromoethane (Aldrich, 99%) were used to synthesize the ionic liquids (ILs). Dichloromethane (Junsei, 99%) and lithium bis(trifluoromethanesulfonyl)imide (TFSI, Morita Chemical Industries Co.) were used for the metathesis reaction of the synthesized ILs. After metathesis, the ILs became TFSI-substituted ion pairs. When the metathesis reaction was complete, several drops of $AgNO_3$ aqueous solution were added to the product to identify whether bromide still remained in the ILs. Final identification of the synthesized IL was performed using nuclear magnetic resonance spectroscopy (NMR, Bruker 400 MHz).

The prepared ILs were characterized as electrolyte components. The electrolytes were evaluated in coin cells. Half-cells containing $LiNi_{0.5}Mn_{1.5}O_4$ (Daejung EM Co. Ltd.) cathode materials were used for the material evaluations. The cathode material was mixed with carbon black (super P black, Timcal Carbon) and polyvinylidene fluoride (PVDF, Aldrich) at a ratio of 87:7:6 in N-methyl-2-pyrrolidone (NMP, Junsei) to create a slurry for the cathode. The slurry was spread on Al foil and dried overnight at 100 °C. The dried electrodes were hot roll-pressed to reduce the thickness by 20%. Lithium foil served as the anode. Two-electrode 2032-type coin cells (Hohsen Corp.) were prepared to monitor the performance of the materials. The diameters of the cathode and anodes were each 15 mm. A 15-μm-thick separator (5301 type, Celgard) was placed between the two electrodes. The electrolytes used for the measurements were prepared by mixing the ILs with a carbonate solvent. The carbonate solvent was ethylene carbonate/diethyl carbonate (EC/DEC) at a ratio of 1:1 by volume (Techno Semichem). $LiPF_6$ was added to the mixed solvent to achieve a final concentration of 1.5 M. The electrolytes were prepared with 1.5 M $LiPF_6$ because a higher concentration of $LiPF_6$ in the electrolyte provides enhanced flame retardancy even though the higher ionic population in the IL can cause a low conductivity [30]. All cell preparations were performed in a dry room. The assembled cells were aged in an oven overnight at 45 °C to accelerate the wetting process in the cells. Following the wetting efforts carried out by aging in the oven, multiple formation cycles at 0.1 C were necessary to establish proper cell operation.

2.2. Instruments and measurements

Prior to the performance measurements, including the rate capability test and the cycle life test, the coin cells were cycled between 3.5 V and 4.9 V at a rate of 0.1 C for 5 formation cycles. A rate of nC yields a full charge (C) in 1/n hours. In the rate capability tests, all charge rates were 0.2 C, except for the 0.1 C discharge test used for the rate capability test, which was charged at 0.1 C. Cycle life tests were carried out at a 0.5 C rate both for charging and discharging. The cell performance was measured using a TOSCAT-2100U cycler (Toyo Systems Co.). Electrochemical impedance spectroscopy (EIS) was performed with a potentiostat (model VSP3, Princeton Applied Research) at the discharge potential (3.5 V) with an AC perturbation of ±10 mV. The frequency range was 0.01 Hz–100 kHz. Conductivity measurements were performed using a conductivity meter (Accumet, XL 20) at room temperature. Either of two conductivity probes (Accumet, cell constants 1.0 cm^{-1} and 10 cm^{-1}) was selected, depending on the conductivity values of the samples. The probes were calibrated with calibration standards (Fisher Scientific) before the measurements were taken. After each use, the probes were cleaned with nitric acid, rinsed with deionized water and dried. The melting points of the ILs were obtained using a differential scanning calorimeter (DSC, Q10, TA instruments). The DSC scans commenced at ambient and then reduced the temperature to −40 °C to freeze the ionic liquids. Phase transitions were observed while the temperature was increased. The DSC scans were carried out at the scan rate of 5 °C min^{-1} under nitrogen. The flame-retardant properties of the mixed electrolytes were evaluated by measuring the self-extinguishing time (SET) normalized by the liquid mass [31,32]. A wide and thin container was used for the burning tests. The container for the SET tests was made of stainless steel and had a diameter of 20 mm and height of 4 mm. The shape of the container allowed for a wide exposure to oxygen and convenience in measuring the weight of the electrolytes. After the electrolytes were carefully ignited, the SET values were measured. Each value was obtained from the average of three measurements.

The results of the ^1H NMR spectroscopy (400 MHz $CDCl_3$) are as follows: 1-methyl-1-propyl piperidinium bis(trifluoromethanesulfonyl) TFSI (MPP-TFSI): δ 1.060 (3H, t, CH_3), 1.760–1.920 (8H, m, ring and $-CH_2-$), 3.063 (3H, s, $N-CH_3$), 3.279 (2H, m, $N-CH_2$), 3.375 (4H, m, $2N-CH_2$); 1-ethyl-1-methyl piperidinium bis(trifluoromethanesulfonyl) TFSI (EMP-TFSI): δ 1.415 (3H, t, CH_3), 1.789

(2H, m, CH_2), 1.921 (4H, m, 2-CH_2), 3.048 (3H, s, N-CH_3), 3.368 (4H, m, 2N—CH_2), 3.279 (2H, q, N—CH_2).

3. Results and discussion

The smallest room-temperature liquid salt among the piperidinium-TFSI ILs is methyl-propyl piperidinium TFSI(MPP-TFSI), the conductivity of which is higher than that of butyl-methyl-piperidinium TFSI because of its smaller cation size, which leads to enhanced mobility in liquids [29,33]. Ethyl-methyl piperidinium TFSI (EMP-TFSI), which is one carbon atom shorter than MPP-TFSI, is solid at RT. Phase transitions of EMP-TFSI were observed in the DSC measurements, as shown in Fig. 1. A glass transition is found at 16.5 °C. EMP-TFSI melts at 85.0 °C, which is 50 °C above room temperature. EMP-TFSI alone cannot be used as the electrolyte solvent. When it is mixed with another liquid solvent, EMP-TFSI can be utilized as a co-solvent in Li-ion batteries. The solid co-solvent, EC, has good permittivity [34] and the ability to form a solid electrolyte interphase (SEI) [35–37], which enables the Li-ion batteries to work longer and more powerfully. EMP-TFSI can be used as a co-solvent with alternative functionality, such as flame retardancy.

Most ILs have lower conductivity values than the carbonate-based electrolytes [25,38]. Unless a drastic decrease in conductivity is caused by the addition of ILs, the mixed IL electrolyte is applicable to Li-ion batteries with moderate discharge rates, which are relevant for energy storage facilities. Fig. 2 shows the conductivity trend when the ILs were mixed with a carbonate electrolyte. The added ILs included MPP-TFSI and EMP-TFSI. The carbonate electrolyte was a 1.5 M solution of EC/DEC (1:1). The change in conductivity was recorded as the IL content was increased. $LiPF_6$ was added to maintain the same Li ion concentration because the IL additions increased the volume of the electrolyte. The lithium salt was well dissolved at a concentration of 1.5 M under our experimental conditions. The only difference between the two solutions was the size of the IL cations. Once the ILs were dissolved in the carbonate electrolyte, the degree of mobility, as affected by the presence of cations, was reflected in the conductivity values. A decrease in the conductivity is proportional to the amount of MPP-TFSI in the solution. However, the conductivity behavior of the EMP-TFSI mixed electrolyte is not directly proportional to the IL content. The rate of decrease of the conductivity with EMP-TFSI is not as high as that with MPP-TFSI. The conductivity values at 30% IL for MPP-TFSI and EMP-TFSI are 3.922 and 5.097 mS cm^{-1}, respectively. EMP-TFSI has a 30% higher value than MPP-TFSI. The value for EMP-TFSI is also higher than that for MPP-TFSI at 50% IL content.

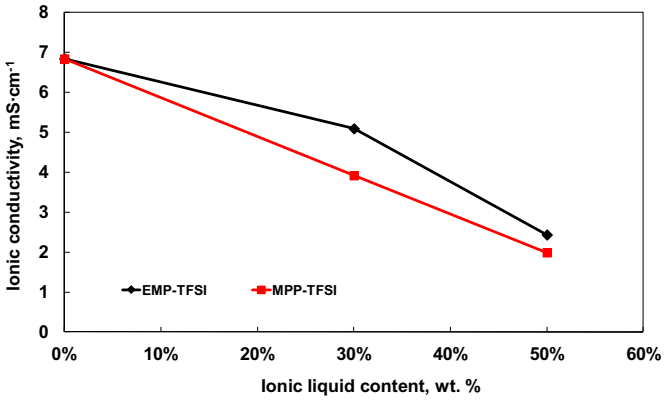

Fig. 2. The conductivity versus the ionic liquid content. The ILs in this case are EMP-TFSI and MPP-TFSI.

The conductivity of EMP-TFSI is 21.9% higher than that of MPP-TFSI. The smaller cation size of EMP-TFSI provides enhanced ionic mobility in the solution in comparison with the larger cation size of MPP-TFSI. The conductivity values with 50% IL are 2 mS cm^{-1} or greater, which is a feasible operational condition for low-discharge Li-ion batteries. The improved ionic conductivity originates from the higher mobility of the smaller cations of EMP-TFSI. However, the higher cationic mobility is not directly related to the enhanced Li^+ mobility, which is an important factor for battery operation. The lithium ion mobility, including other over-potential elements, can be evaluated indirectly by performing cell tests.

The flame retardant properties of the mixed IL solutions were evaluated by measuring the SET value shown in Fig. 3. A shorter extinction time indicates stronger flame retardancy. The mixed solutions were burned to obtain SET values with respect to IL contents. The addition of 30% IL shortens the extinction time by 31.8% and 39.1% for solutions of MPP-TFSI and EMP-TFSI, respectively. The extinction time is 14.2 s for EMP-TFSI and 1.0 s for MPP-TFSI with a 50% IL addition. The addition of 50% IL produces a nonflammable solution with MPP-TFSI and a flame-retardant solution with EMP-TFSI. The 50% IL solution with EMP-TFSI exhibits reasonable conductivity and good fire resistance [32].

Because the 50% IL solutions provide sufficiently high conductivity for use in slow discharge conditions, the battery performance tests were conducted with the 50% IL solutions. The electrode materials used in the battery tests were natural graphite and $LiNi_{0.5}Mn_{1.5}O_4$ as the anode and cathode materials, respectively. Half-cells were assembled for each electrode material. The natural

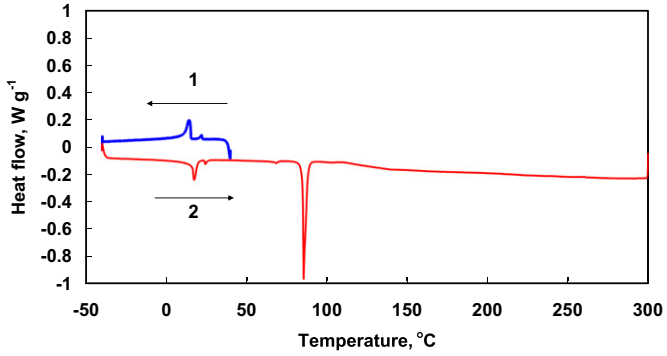

Fig. 1. The DSC measurements with EMP-TFSI. The temperature scan was carried out from room temperature to the cooling cycle. The phase transition temperatures were determined during the heating cycle. Numbers 1 and 2 and the arrows represent the direction of the temperature scan.

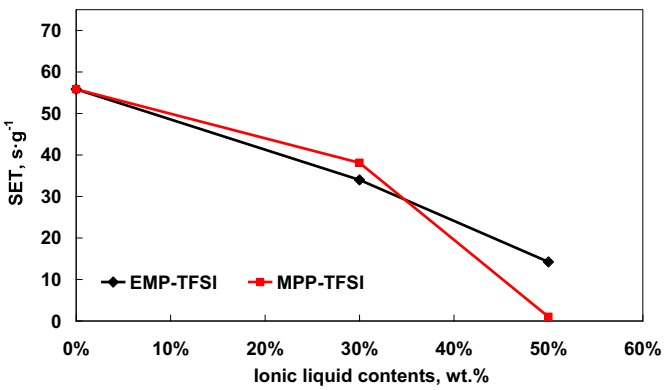

Fig. 3. The SET value versus the ionic liquid content. The ILs in this case are EMP-TFSI and MPP-TFSI.

graphite electrodes only survived for approximately 5 cycles (not shown here). Thus, graphite electrodes are not suitable for use in these ILs or IL mixed electrolytes [4,19]. Additives that form protective layers on graphite should be used to extend the cycle life of graphite electrodes [16,22]. Additive studies and anode selections are not discussed in this paper.

The charge and discharge voltage profiles with $LiNi_{0.5}Mn_{1.5}O_4$ were obtained with rates of 0.2 and 1.0 C, respectively, as shown in Fig. 4. Two IL-mixed electrolytes and the pure carbonate electrolyte were compared in the cell tests. Under the slow charge and discharge conditions, the influence of the conductivity on the discharge capacities is not significant. The discharge capacity values are comparable in all electrolytes. Although the conductivity value is not the only element that determines cell performance, the conductivity values of the electrolytes are found to have an influence on the voltage profiles by way of over-potentials. The relative intensity of the over-potential can be compared between the charge and discharge plateaus. As the depth of the charge and discharge states increases, the potential gap in each cell becomes more pronounced. The electrolyte with the lowest conductivity, the MPP-TFSI mixed solution, demonstrates the largest over-potential among the tested electrolytes. The conductivity values are directly related to the IR drop. However, the over-potentials are the combined values of the IR drop, the mass-transfer, the activation energy, and the charge transfer elements in both IL-mixed electrolytes. The influence of the conductivity on the IR drop can be separated from other over-potentials by performing discharge tests at a variety of current values.

As the discharge rate increases, the IL with a slightly lower conductivity more negatively affects the discharge capacities of the electrodes. The discharge capacities versus the discharge rate (the rate capability tests) are shown in Fig. 5. All of the electrolytes demonstrate similar discharge conditions on the $LiNi_{0.5}Mn_{1.5}O_4$ electrode up to a rate of 1.0 C. The electrodes in both the pure carbonate electrolyte and the EMP-TFSI mixed electrolyte discharged 97% of the charged capacity at 1.0 C. The MPP-TFSI mixed solution allows for a discharge efficiency of 92%. The discharge capacities and efficiencies diverges at discharge rates higher than 1.0 C. Compared with the other electrolytes, the mixed electrolyte of MPP-TFSI damages the discharge values substantially at discharge rates of 2.0 and 5.0 C. The low ionic conductance of the mixed electrolyte and the other over-potential elements of MPP-TFSI are not favorable at high discharge rates. Additionally, the capacity of the cell with the EMP-TFSI mixed electrolyte at 5.0 C is slightly improved compared with that of the carbonate electrolyte. This finding implies that the conductivity is not the only factor that

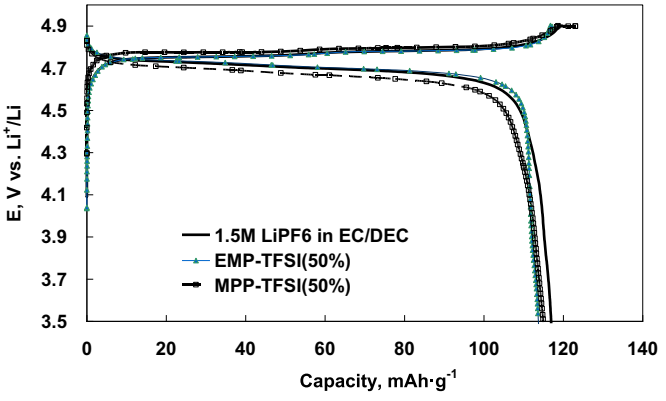

Fig. 4. The discharge capacity values with 50% ILs and a pure carbonate electrolyte. Prior to the measurements, 5 formation cycles at a rate of 0.1 C were performed for each measurement. The charge and discharge rates were 0.2 and 1.0 C, respectively.

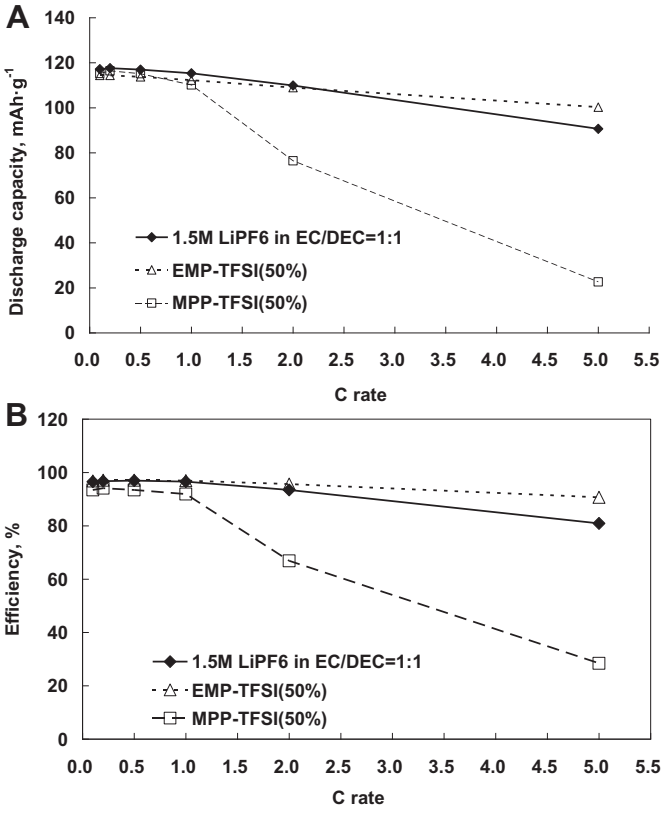

Fig. 5. The rate capability tests with 50% ILs and a pure carbonate electrolyte: (a) the discharge values versus the discharge rate and (b) the coulombic efficiency versus the discharge rate. Prior to the measurements, 5 formation cycles at a rate of 0.1 C were performed for each measurement. The measurements started at a slow discharge rate and were increased. The discharge rates were 0.1, 0.2, 0.5, 2.0 and 5.0 C.

determines the cell performance values. The discharge capacity values with EMP-TFSI are slightly lower than those with the pure carbonate electrolyte at low discharge rates, as shown in Fig. 5A. In Fig. 5B, it can be observed that the coulombic efficiencies of the cell with EMP-TFSI were almost steady, while the efficiency of the cell with the carbonate electrolyte declines as the discharge rate was increased. Although the EMP-TFSI mixed electrolyte exhibits a lower conductivity than the pure electrolyte, the discharge condition improves, which results in an increased efficiency.

The cycle life tests evaluate the durability of the mixed IL as a potential electrolyte for use in Li-ion batteries. Charge and discharge cycles at rates of 0.5 C were performed. Fig. 6A shows the discharge capacities of the $LiNi_{0.5}Mn_{1.5}O_4$ electrodes during the cycle tests, which were carried out in three electrolytes. All of the electrodes in each of the three electrolytes maintain their capacity over 50 cycles. Both the carbonate and EMP-TFSI mixed electrolytes provided steady capacities at every cycle until the end of the test. However, the capacity values from the electrode in MPP-TFSI are unstable, even though the capacity level is similar to that of the other electrodes. The mixed electrolytes perform very well under the slow discharge rates. The capacity retention results shown in Fig. 6A indicate that the mixed electrolytes are electrochemically stable for use in high-voltage cathode materials under half-coin cell operating conditions. The coulombic efficiency values of cycle life tests, which are shown in Fig. 6B, can be used to evaluate the electrolyte decomposition. A low coulombic efficiency value is an indirect indication of electrolyte decomposition because the capacity values of all electrolytes are comparable. The pure carbonate and EMP-TFSI electrolytes are stable and exhibit comparable results. However, the efficiency values of the MPP-TFSI electrolyte are unstable and

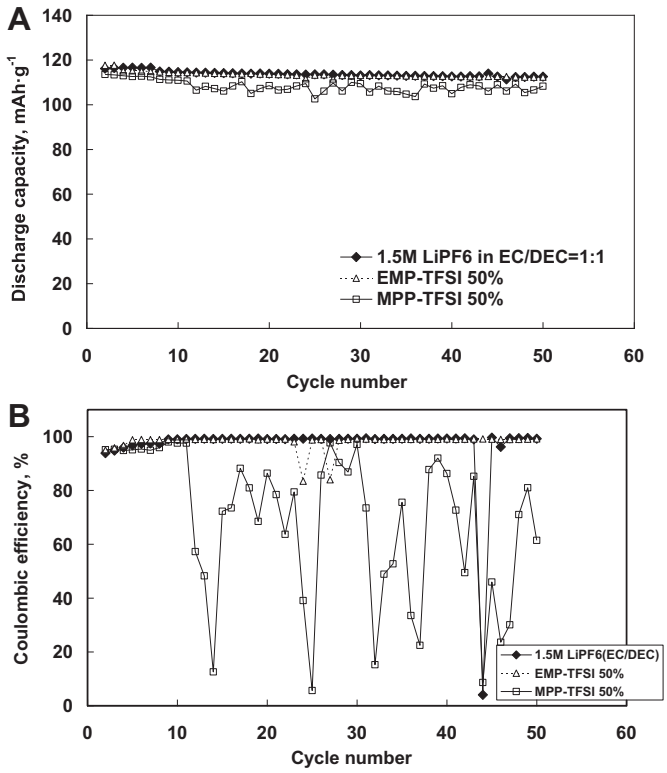

Fig. 6. The cycle life tests with 50% IL and a pure carbonate electrolyte. Both the charge and discharge rates for the tests were 0.5 C.

significantly lower than those of the other two electrolytes. This result implies that the oxidation reaction of the MPP-TFSI mixed electrolyte is more active than the reaction of the other two solutions. The candidates for undergoing oxidation in the mixture are carbonate molecules. However, neither the mechanism of reduced stability in the MPP-TFSI mixed solution nor the types of elements in the mixture that are more active during oxidation is known at this point. Further studies will be carried out to understand the stability of mixed ILs.

Changes in the resistive elements during the cycle life tests were monitored with EIS measurements. The spectra were recorded after the 3rd and 50th cycles at the discharged state during the cycle life tests. The spectra at the 3rd cycle (Fig. 7A) essentially consist of two semi-circles followed by a corresponding low-frequency inclined line; however, in the case of the EMP-TFSI in which only one semi-circle appears, while the spectra at the 50th cycle (Fig. 7B) is comprised of one semi-circle and a subsequent inclined line. The semi-circle(s) is attributed to the SEI film and charge transfer resistances, and the inclined line is the result of diffusion behavior. Single semi-circle behavior of the spectra is most likely due to the proximity of the reaction time constants in the SEI film and the combined reaction of charge transfer and double layer charging/discharging. In light of this, we constructed two types of equivalent circuits to model the pair and individual semi-circle behaviors, as shown in the insets of Fig. 7A and B, respectively. In the circuits, R_Ω, R_f, and R_{ct} are the bulk electrolyte resistance, the surface film resistance, and the charge transfer resistance, respectively, and R_{comb} is the summation of R_f and R_{ct}. The CPE_f and CPE_{dl} denote the constant phase elements caused by the capacitive behaviors of the film and the double layer, respectively, while the CPE_{diff} is the constant phase element coming from the solid-state diffusion process. The resistance values were determined from the complex non-linear least squares (CNLS) fits of the spectra to the corresponding equivalent circuits, as listed in Table 1.

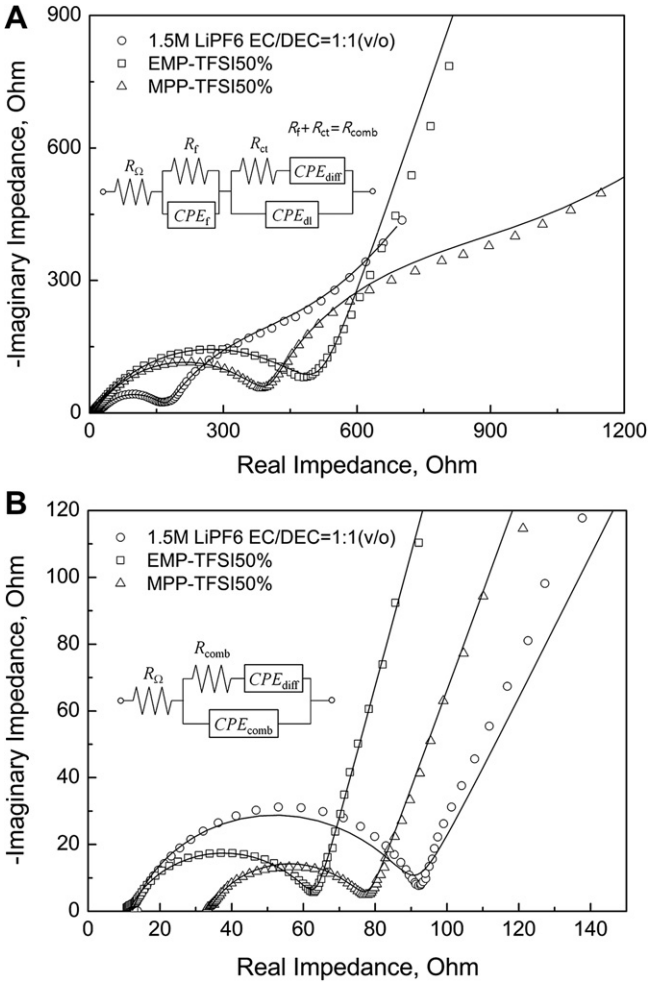

Fig. 7. The EIS spectra after the (a) 3rd and (b) 50th cycles. The equivalent circuits used to model the spectra are given in the insets. The solid lines were determined by the CNLS fittings of the spectra to the equivalent circuits.

Because electrodes at early cycles still experience wetting and surface film formation processes, the resistance values at these cycles are significantly higher than those from electrodes that have completed the cycles [39]. The contribution of wetting to the impedance is possibly included in R_{ct}. The cells with the mixed IL solutions have higher viscosities than the cell with the pure carbonate solution. The higher solution viscosity causes a slow wetting process and affects the charge transfer resistance. After 50 cycles, the resistance values of the cells with the IL mixed solutions are significantly lower than those of the 3rd cycles, as shown in Fig. 7B. At this point, the cell wetting and film formation processes are nearly complete, which provides steady state conditions for the continuous cycles. The total impedance values for all of the cells are

Table 1
The elementary cell resistances in different electrolytes, determined from the CNLS fittings of the impedance spectra to the equivalent circuits (Fig. 7A and B).

1 M $LiPF_6$ EC/DEC				EMP-TFSI50%				MPP-TFSI50%			
3rd cycle											
R_Ω	R_f	R_{ct}	R_{comb}[a]	R_Ω	R_f	R_{ct}	R_{comb}[b]	R_Ω	R_f	R_{ct}	R_{comb}[a]
19.4	155.1	500.2	655.3	7.2	–	–	524.5	9.8	401.2	612.5	1.14k
50th cycle											
R_Ω	R_f	R_{ct}	R_{comb}[b]	R_Ω	R_f	R_{ct}	R_{comb}[b]	R_Ω	R_f	R_{ct}	R_{comb}[b]
12.3	–	–	78.9	11.3	–	–	52.6	33.6	–	–	44.8

[a] Calculated from the equation $R_{comb} = R_f + R_{ct}$.
[b] Estimated from the impedance spectra by CNLS fittings.

not sufficiently distinct to cause differences in values in the cycle life tests.

The R_{comb} of the cell using EMP-TFSI is slightly lower than that of the pure carbonate electrode. The low R_{comb} can provide increased performance in some discharge conditions. However, there is no difference in the cycle life results tested at a slow discharge rate of 0.5 C. The discharge capacity values at higher discharge rates are affected by the low resistance values (R_{comb}), as shown in Fig. 5. The cell using the EMP-TFSI mixed solution shows a slightly higher discharge capacity at 5.0 C than the cell with the pure carbonate solution, which results from the steady discharge coulombic efficiency at all discharge rates. A comparison of Fig. 7A and B demonstrates that the change in R_{Ω} of the cell using MPP-TFSI is significantly higher than that of the other cells. The R_{Ω} value is increased approximately three-fold after 50 cycles, which results in the unstable capacity values in the cycle life tests. The increase in the electrolyte resistance after multiple cycles suggests that the electrolyte is somehow consumed in the cycling process, which hinders ionic movement during subsequent redox activities. The decomposition of the MPP-TFSI mixed electrolyte was monitored in Fig. 6B as well. Slow discharge rates (less than 2.0 C) had almost no effect on the capacity values, as shown in Fig. 5, which corresponds to the comparable discharge capacity values in the cycle life test.

4. Conclusions

Even though the presence of smaller cations in ionic liquids leads to increased melting points in comparison with ionic liquids with larger cations, the small cations provide enhanced ionic conductivity when they are dissolved in other liquid solvents. EMP-TFSI provides better conductivity than MPP-TFSI in solution because of its smaller cationic size. The EMP-TFSI mixed electrolyte leads to enhanced over-potentials versus the MPP-TFSI mixed electrolyte in battery operations. The advantages of improved conductivity, over-potentials, and durability further enhanced the redox reaction rates in the Li-battery operation. The 50% EMP-TFSI mixed electrolyte performed as well as the pure carbonate electrolyte. Additionally, the cycle life results for this electrolyte are comparable to those of the pure carbonate electrolyte. Thus, ILs with melting temperatures above room temperature can perform very well as mixed electrolytes. Additionally, a 50% mixture of IL can provide enhanced safety.

Acknowledgments

This work was supported by the National Research Foundation of Korea Grant funded by the Ministry of Education, Science and Technology (MEST) of the Korean Government (NRF-2009-C1AAA001-2009–0093307). This research was also supported by MEST (NRF-2012-R1A1A2-006562).

References

[1] C.H. Patrick, R.M. Douglas, F.H. Anthony, Electrochem. Solid-State Lett. 7 (2004) A97–A101.
[2] S. Seki, Y. Kobayashi, H. Miyashiro, Y. Ohno, A. Usami, Y. Mita, N. Kihira, M. Watanabe, N. Terada, J. Phys. Chem. B 110 (2006) 10228–10230.
[3] B. Garcia, S. Lavallee, G. Perron, C. Michot, M. Armand, Electrochim. Acta 49 (2004) 4583–4588.
[4] H. Zheng, B. Li, Y. Fu, T. Abe, Z. Ogumi, Electrochim. Acta 52 (2006) 1556–1562.
[5] H. Sakaebe, H. Matsumoto, Electrochem. Commun. 5 (2003) 594–598.
[6] H. Matsumoto, H. Sakaebe, K. Tatsumi, J. Power Sources 146 (2005) 45–50.
[7] M. Ishikawa, T. Sugimoto, M. Kikuta, E. Ishiko, M. Kono, J. Power Sources 162 (2006) 658–662.
[8] S.S. Jeong, N. Bockenfeld, A. Balducci, M. Winter, S. Passerini, J. Power Sources 199 (2012) 331–335.
[9] H. Kim, M. Ding, A.P. Kohl, J. Power Sources 198 (2012) 281–286.
[10] G.T. Kim, S.S. Jeong, M.Z. Xue, A. Balducci, M. Winter, S. Passerini, F. Alessandrini, G.B. Appetecchi, J. Power Sources 199 (2012) 239–246.
[11] R.D. Rodgers, K.R. Seddon, Science 302 (2003) 792–793.
[12] M. Galinski, A. Lewandowski, I. Stepniak, Electrochim. Acta 51 (2006) 5567–5580.
[13] A. Guerfi, M. Dontigny, P. Charest, M. Petitclerc, M. Lagace, A. Vijh, K. Zaghib, J. Power Sources 195 (2010) 845–852.
[14] J.K. Kim, A. Matic, J.H. Ahn, P. Jacobsson, J. Power Sources 195 (2010) 7639–7643.
[15] S. Fang, Z. Zhang, Y. Jin, L. Yang, S.I. Hirano, K. Tachibana, S. Katayama, J. Power Sources 196 (2011) 5637–5644.
[16] T. Sato, T. Maruo, S. Marukane, K. Takagi, J. Power Sources 138 (2004) 253–261.
[17] M. Holzapfel, C. Jost, P. Novak, Chem. Commun. (2004) 2098–2099.
[18] H. Zheng, K. Jiang, T. Abe, Z. Ogumi, Carbon 44 (2006) 203–210.
[19] V. Baranchugov, E. Markevich, G. Salitra, D. Aurbach, G. Semrau, M.A. Schmidt, J. Electrochem. Soc. 155 (2008) A217–A227.
[20] J. Reiter, M. Nadherna, EleCtrochim. Acta 71 (2012) 22–26.
[21] T. Yim, Y.L. Hyun, H.J. Kim, J. Mun, S. Kim, S.M. Oh, G.K. Young, Bull. Korean Chem. Soc. 28 (2007) 1567–1572.
[22] X.G. Sun, S. Dai, Electrochim. Acta 55 (2010) 4618–4626.
[23] C.S. Stefan, D. Lemordant, B. Claude-Montigny, D. Violleau, J. Power Sources 189 (2009) 1174–1178.
[24] V. Borgel, E. Markevich, D. Aurbach, G. Semrau, M. Schmidt, J. Power Sources 189 (2009) 331–336.
[25] K. Liu, Y.X. Zhou, H.B. Han, S.S. Zhou, W.F. Feng, J. Nie, H. Li, X.J. Huang, M. Armand, Z.B. Zhou, Electrochim. Acta 55 (2010) 7145–7151.
[26] M. Rao, X. Geng, Y. Liao, S. Hu, W. Li, J. Membr. Sci. 399-400 (2012) 37–42.
[27] J. Reiter, M. Nadherna, R. Dominko, J. Power Sources 205 (2012) 402–407.
[28] Y.Y. Cheng, C.C. Li, J.T. Lee, Electrochim. Acta 66 (2012) 332–339.
[29] M. Kunze, E. Paillard, S. Jeong, G.B. Appetecchi, M. Schonhoff, M. Winter, S. Passerini, J. Phys. Chem. C 115 (2011) 19431–19436.
[30] A. Fernicola, F. Croce, B. Scrosati, T. Watanabe, H. Ohno, J. Power Sources 174 (2007) 342–348.
[31] Y.H. Cho, K. Kim, S. Ahn, H.K. Liu, J. Power Sources 196 (2011) 1483–1487.
[32] K. Xu, M.S. Ding, S. Zhang, J.L. Allen, T.R. Jow, J. Electrochem. Soc. 149 (2002) A622–A626.
[33] J. Salminen, N. Papaiconomou, R.A. Kumar, J.M. Lee, J. Kerr, J. Newman, J.M. Prausnitz, Fluid Phase Equilib. 261 (2007) 421–426.
[34] D.R. Lide (Ed.), Handbook of Chemistry and Physics, eightyninth edition, CRC Press, Florida, 2008.
[35] T. Piao, S.-M. Park, C.-H. Doh, S.-I. Moon, J. Electrochem. Soc. 146 (1999) 2794.
[36] R. Yazami, Electrochim. Acta 45 (1999) 87.
[37] N. Takami, A. Satoh, M. Hara, T. Ohsaki, J. Electrochem. Soc. 142 (1995) 371–379.
[38] G.-A. Nazri, G. Pistoia (Eds.), Lithium Batteries: Science and Technology, Kluwer Academic Publishers, Nowell, 2004.
[39] K. Kim, S. Ahn, H.S. Kim, H.K. Liu, Electrochim. Acta 54 (2009) 2259–2265.